Review

Benign liver lesions: grey-scale and contrast-enhanced ultrasound appearances

A E Obaro and S M Ryan

Department of Radiology, King's College Hospital NHS Foundation Trust, Denmark Hill, London, UK
Corresponding author: S M Ryan. Email: suzanneryan@nhs.net

Abstract

Ultrasound is often the first point of detection of liver lesions, with up to 75% of liver lesions detected at ultrasound having benign histology. In 2012, NICE issued recommendations that ultrasound contrast be used for the evaluation of incidentally discovered liver lesions. This has been demonstrated to provide a rapid and cost-effective evaluation for incidental liver lesions, in many cases precluding the need for further CT or MRI scans. The aim of this review is to demonstrate the ultrasound features of benign liver lesions, and to demonstrate their further characterisation with contrast ultrasound.

Keywords: Benign liver lesions, contrast-enhanced ultrasound, grey-scale ultrasound

Ultrasound 2015; **23**: 116–125. DOI: 10.1177/1742271X15575805

Introduction

Contrast-enhanced ultrasound (CEUS) is the only truly intravascular non-interventional contrast medium, and allows angiographic evaluation of the enhancement characteristics of liver lesions. Ultrasound contrast agents are gas-filled microbubbles (typically 3 µm in diameter) that are administered intravenously to the systemic circulation. These microbubbles resonate in an ultrasound beam, rapidly contracting and expanding in response to the pressure changes of the sound wave. This makes them several thousand times more reflective than normal body tissues. In this way, they enhance both grey-scale images and flow mediated Doppler signals.[1]

Ultrasound contrast agents allow the liver to be evaluated in three phases. The first is the arterial phase which occurs at 10–35 seconds after injection and gives information regarding the arterial supply of a lesion. The second, the porto-venous phase, 30–120 seconds, allows assessment of 'washout' of lesions. The third phase is a delayed phase occurring beyond 120 seconds and this allows for cell uptake or sinusoidal pooling to be assessed. Microbubble disappearance occurs at between 240 and 360 seconds.[2]

For evaluation of liver lesions with contrast ultrasound, 2.4 mL of contrast is injected intravenously followed by 10 mL of saline flush. A low mechanical index (MI) of 0.1–0.2 is used to ensure minimal microbubble destruction. Once the target lesion is scanned in contrast-specific mode, ideally with a parallel B-mode image, the timer should be started to allow accurate timing assessment of enhancement patterns. Bubbles can be 'burst' by applying a short pulse high MI scan through the lesion, or another dose of contrast agent can be given to re-assess the vascular characteristics of lesions, if there is initial uncertainty with the diagnosis.[2]

It is estimated that the cost of the CEUS examination, if performed during the same sitting as a B-mode ultrasound, is £65; a contrast CT examination would cost between £116 and £162 and a contrast MR examination between £189 and £366.[3]

NICE guidelines state that 75% of incidentally detected liver lesions are benign. In our practice, microbubble contrast is used as a problem-solving tool. We run dedicated CEUS lists which allow us to confidently identify benign lesions and exclude or refer on malignant lesions. Clinical information is also considered and may be directive particularly in the presence of sepsis. The most commonly encountered benign liver lesions will be discussed with the CEUS imaging characteristics.

Cavernous haemangioma

These are the most common benign liver lesions with a prevalence of between 1.4% and 20%, with multiple lesions occurring in 9–22% of patients.[4,5] At ultrasonography (US), the typical appearance is a homogeneous, hyperechoic mass with well-defined margins and posterior acoustic enhancement.[6] Despite their vascularity, Doppler flow is not useful as flow within the lesion is too slow to be detected by Doppler. Contrast ultrasound demonstrates globular peripheral centripetal enhancement, with progressive infilling (Figure 1(a) and (b)). This is particularly useful in the presence of atypical haemangiomas, which appear on

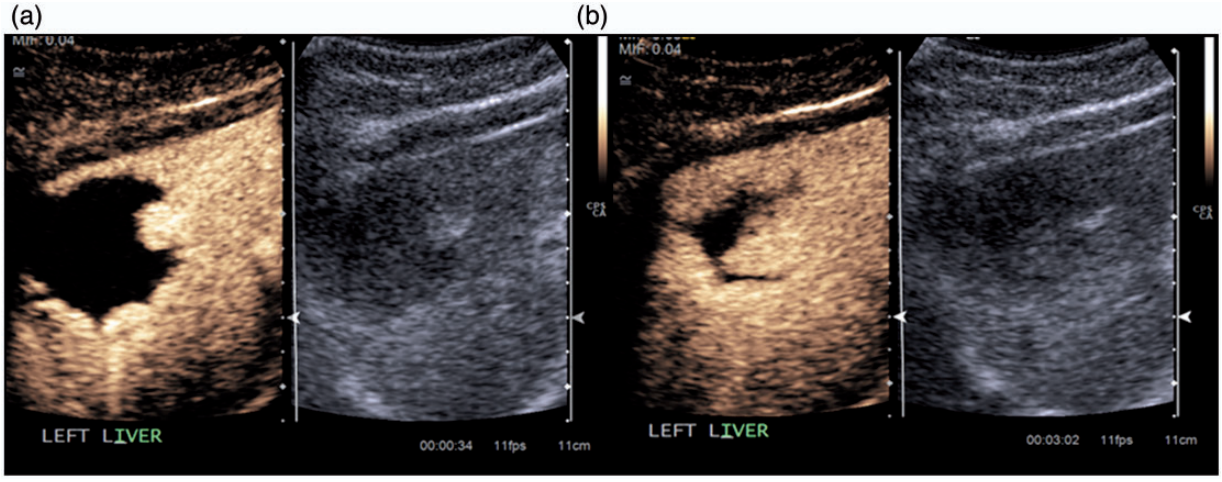

Figure 1. Haemangioma demonstrating: (a) early and (b) late centripetal filling

baseline examinations as hypo- or isoechoic (having the same echogenicity as the surrounding liver parenchyma, commonly with a thin hypoechoic peripheral rim).[6]

Atypical haemangiomas may have a thick hyperechoic rind or a thin hyperechoic rim, with an internal echo pattern that is at least partially hypoechoic.[6,7] Large haemangiomas (termed giant haemangiomas when they exceed 4 cm in diameter) are often heterogeneous.[6–10] Larger lesions will have an initial similar enhancement pattern with centripetal progression but they do not completely fill centrally due to their large size. Smaller capillary haemangiomas /rapidly filling haemangiomas are not very frequent (16% of all haemangiomas).[7]

Rapid filling occurs more often in small haemangiomas.[11] Evaluation with CEUS demonstrates immediate homogeneous enhancement at arterial phase. An important differential is hypervascular metastases, or in the correct clinical context hepatocellular carcinoma (HCC). Accurate diagnosis is made with delayed-phase imaging because haemangiomas remain hyperattenuating or hyperintense, whereas hypervascular metastases do not, and most moderately differentiated HCCs will show portal venous washout.[12] In our practice CEUS is performed in all incidentally detected benign lesions, unless they are inaccessible to ultrasound or less than 5 mm in size.

Focal fat deposition and focal sparing

Fatty infiltration of the liver represents abnormal triglyceride uptake within hepatocytes and may be either diffuse or focal. Focal infiltration is commonly associated with alcohol abuse and morbid obesity, but can also be seen with diabetes mellitus, pregnancy, steroid therapy, chemotherapy, malnutrition and hyperalimentation. Focal fat infiltration is assumed to be related to regional perfusional differences or disturbances in hepatic portal blood flow.[2,13,14] Focal fat deposition or focal fat sparing characteristically occurs in specific areas, adjacent to the falciform ligament or ligamentum venosum, in the porta hepatus or gallbladder fossa, within the anterior aspect of the medial segment of the left lobe of the liver (segment IV), or anterior to the portal vein bifurcation.[4] The absence of a mass effect on vessels and other liver structures is also suggestive of fatty infiltration rather than a true lesion. However, when focal fat infiltration presents in a nodular form, diagnosis can be difficult. The differential diagnosis includes other hyperechoic hepatic lesions, such as hyperechoic metastases, haemangioma, FNH and adenoma. In this instance CEUS can be useful.

Administration of contrast material allows a confident diagnosis to be made, as the enhancement pattern is similar to or less than that of the normal liver parenchyma, with no mass lesion demonstrated (Figure 2).

Cystic lesions

Benign developmental hepatic cyst

Benign developmental hepatic cyst is the second most common benign hepatic lesion (after cavernous haemangioma), present in 2.5% of the population,[15] more commonly found in women than men and usually asymptomatic.[15–17] Benign hepatic cyst is a congenital lesion derived from biliary endothelium that does not communicate with the biliary tree. Cysts can be solitary or multiple, and are typically discovered incidentally in the fifth to seventh decades of life and are typically round or ovoid and well defined.[18] The B-Mode ultrasound appearances are of a hypoechoic lesion with posterior acoustic enhancement. A simple cyst will not enhance post contrast administration (Figure 3). In our practice, contrast is used in selected cases e.g. on a background of malignancy, to exclude small metastases. A differential for benign cystic lesion would include hepatic metastases, some of which may appear cystic due to necrosis and cystic degeneration of rapidly growing hypervascular metastases.

On CEUS, cystic metastases appear as solitary or, more commonly, multifocal lesions with complex features, such as thick, irregular, enhancing walls, thick or nodular enhancing septations, enhancing mural nodularity or internal debris.

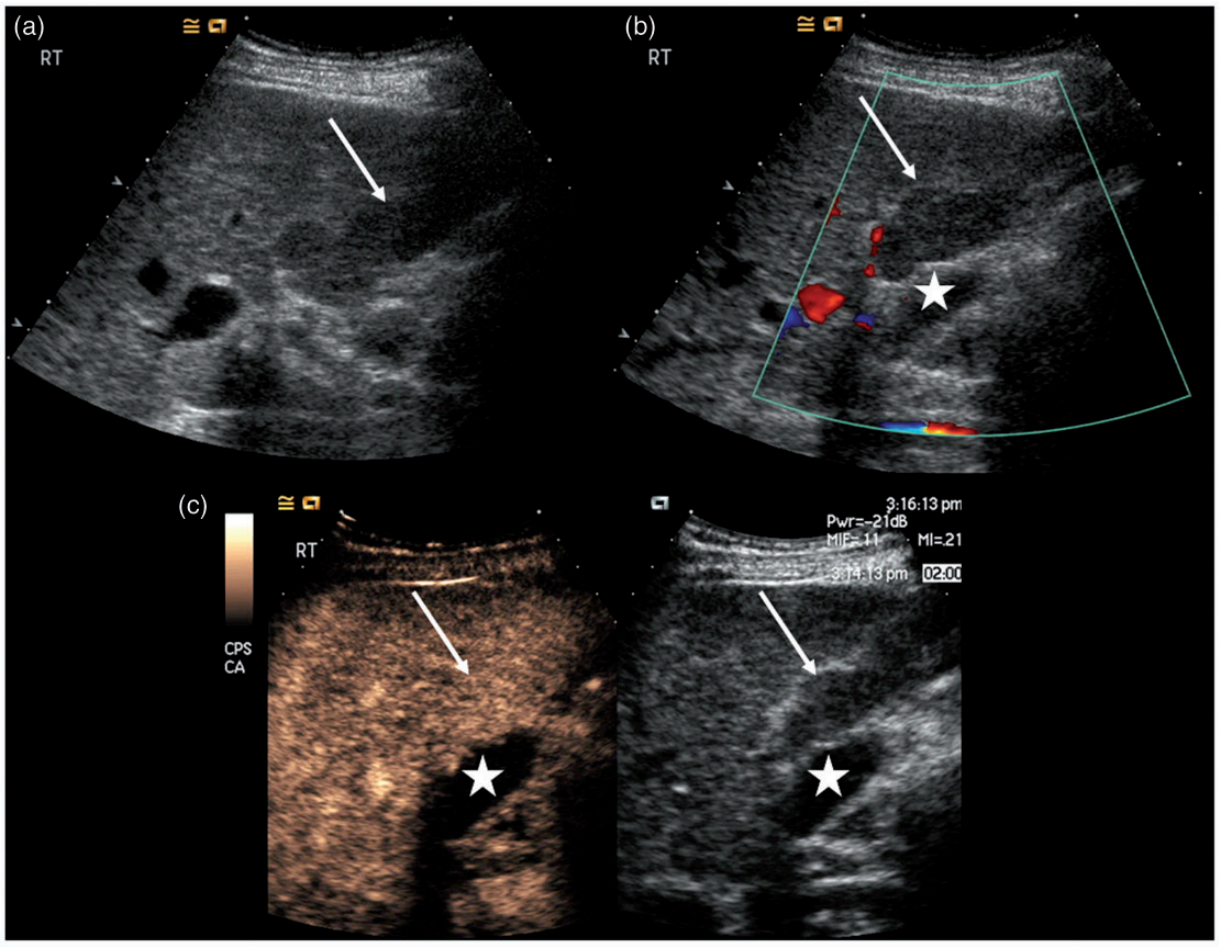

Figure 2. Focal fatty sparing on: (a) grey scale, (b) colour Doppler and (c) CEUS (arrow = focal fatty sparing, star = gallbladder fossa). Focal fatty sparing is isoechoic to background liver on administration of ultrasound contrast (c)

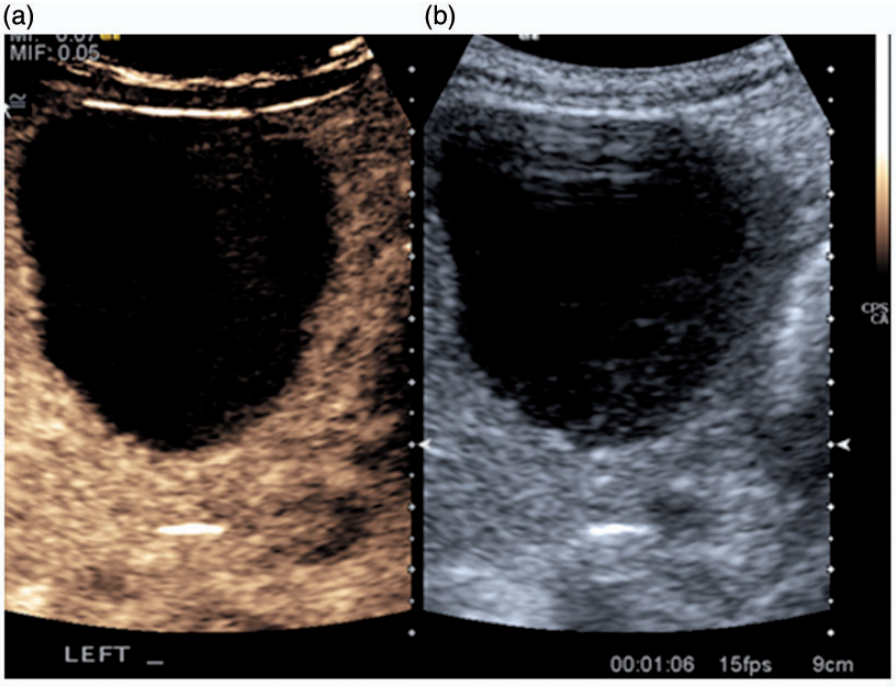

Figure 3. Simple cyst on (a) CEUS and (b) grey scale

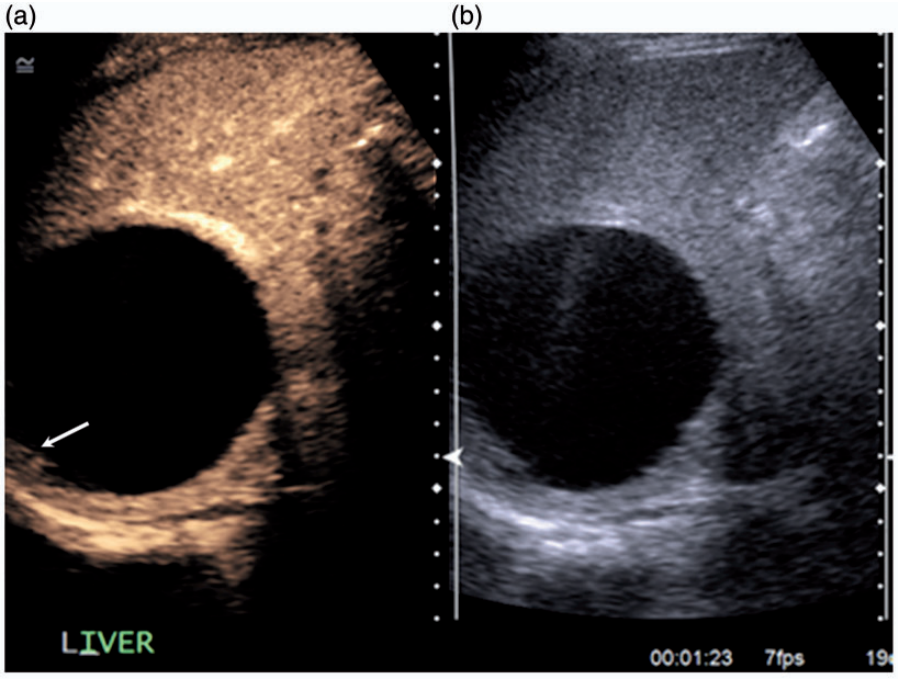

Figure 4. Histologically proven biliary cystadenoma on: (a) CEUS and (b) grey scale. Note the subtle enhancing mural nodularity (arrow)

Complicated infectious and hemorrhagic cysts

Infection or hemorrhage into a simple hepatic cyst results in the development of a complex cystic lesion, which may be indistinguishable from a cystic tumour. Unlike simple cysts, infected or hemorrhagic livers cysts present clinically with pain and fever.

On ultrasound, hemorrhagic cysts appear as hypoechoic lesions with increased through transmission and lack of internal vascularity.[18] On CEUS, the characteristic appearance is of a complex cystic lesion with variable features, which may range from cysts with internal hemorrhagic components to more complex cystic masses with a thick well-defined fibrous capsule, internal septations and mural nodularity. The appearance may mimic biliary cystadenoma or biliary cystadenocarcinoma. The fluid component in an infected or hemorrhagic cyst does not show any contrast enhancement, whereas solid areas in malignancy will demonstrate enhancement.

Biliary cystadenoma and biliary cystadenocarcinoma

Biliary cystadenoma and biliary cystadenocarcinoma are premalignant and malignant cystic biliary ductal neoplasms, respectively, that account for fewer than 5% of intrahepatic cystic lesions of biliary origin. They arise mainly from the intrahepatic ducts and rarely from the extrahepatic ducts or gallbladder. These neoplasms are most frequently found within the right lobe of the liver (55%) but also may involve the left (29%) or both lobes (16%). Biliary cystadenomas range in diameter from 1.5 to 35 cm.[18] Biliary cystadenoma presents predominantly in middle-aged white women with abdominal pain, nausea, vomiting, and obstructive jaundice. They are considered premalignant lesions.

The characteristic ultrasound appearance is a solitary complex cystic mass with a well-defined thick fibrous capsule, internal septations, mural nodularity and, occasionally, capsular calcification (Figure 4).[18] The key difference between biliary cystadenoma or biliary cystadenocarcinoma and a hemorrhagic or infected hepatic cyst is that the capsule, internal septations and mural nodules show contrast enhancement in the former and do not in the latter.[18] Polypoid, pedunculated excrescences are more likely to be seen in biliary cystadenocarcinoma than in cystadenoma, although papillary areas and polypoid projections have been reported in benign cystadenomas.[18,19] The purpose of CEUS in this context would be to direct further imaging/management.

Bile duct hamartoma / von Meyenberg complex

These are benign developmental malformations composed of dilated intrahepatic bile ductules embedded in fibrous stroma.[20] The prevalence on autopsy ranges from 0.6 to 2.8%.[20] In clinical practice, the majority are discovered incidentally, but may present a diagnostic dilemma when the patient is undergoing staging imaging for known primary malignancy.[21]

Sonographic appearances are varied, being described as multiple hypoechoic lesions, hyperechoic lesions and also a mixture of both hypo- and hyperechoic lesions.[21] Other features include the presence of a comet tail artefact demonstrated on ultrasound[20] and there is a documented association with liver cysts. Berry et al.[22] reported a case of multiple biliary hamartomas that did not demonstrate

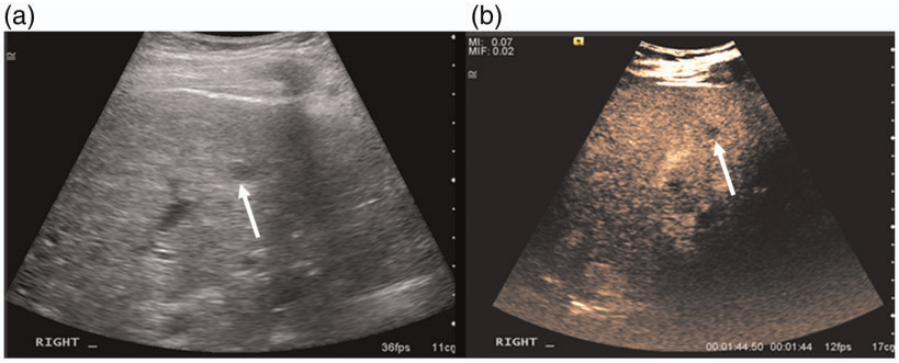

Figure 5. von Meyenburg complex on: (a) grey scale and (b) CEUS (white arrow)

contrast enhancement in all phases of contrast ultrasound (Figure 5).

CT studies have demonstrated variable patterns of enhancement. Although homogeneous enhancement of the lesions has been noted in some cases, in most reports no enhancement was seen on contrast-enhanced CT images.[23–25] Multiple small (<1.5 cm diameter) cystic lesions in the liver without renal involvement should favour the diagnosis of biliary hamartomas.[18]

Intrahepatic hydatid cyst

The right lobe is the most frequently involved portion of the liver with hydatid infection. The US appearance of hydatid cysts may vary. The cyst wall usually manifests as double echogenic lines separated by a hypoechoic layer.[26] Simple cysts do not demonstrate internal structures, although multiple echogenic foci due to hydatid sand may be seen.[27] Complete detachment of the membranes inside the cyst has been referred to as the US water lily sign because of its resemblance to the radiographic water lily sign in pulmonary cysts.[26,28] US is the most sensitive modality for the detection of membranes, septa and hydatid sand within the cyst.[26]

Multivesicular cysts manifest as well-defined fluid collections in a honeycomb pattern with multiple septa representing the walls of the daughter cysts.[29] Daughter cysts appear as cysts within a cyst. When daughter cysts are separated by the hydatid matrix (a material with mixed echogenicity), they demonstrate a 'spoke wheel' pattern.[30] The matrix represents hydatid fluid containing membranes of broken daughter vesicles, scolices and hydatid sand. Membranes may appear within the matrix as serpentine linear structures, a finding that is highly specific for hydatid disease.[26,30] When the matrix fills the cyst completely, a mixed echogenic pattern is created that mimics a solid mass (Figure 6).[28,30,31]

Cyst calcification usually occurs in the cyst wall, although internal calcification in the matrix may also be seen. US demonstrates a hyperechoic contour with a cone-shaped acoustic shadow.[31] When the cyst wall is heavily calcified, only the anterior portion of the wall is visualised and appears as a thick arch with a posterior concavity.[31] Partial calcification of the cyst does not always indicate the death of the parasite; nevertheless, densely calcified cysts may be assumed to be inactive.[27,32] There is little data in the published literature on the CEUS appearances of hydatid disease. Peripheral enhancement of the surrounding liver parenchyma has been demonstrated on contrast-enhanced CT, with wall enhancement in the presence of surrounding abscesses.[33]

Solid lesions

Focal nodular hyperplasia

FNH is a benign lesion due to proliferation of normal non-neoplastic hepatocytes that are abnormally arranged; it is frequently associated with a central stellate area of fibrosis and anomalous arteries.[34] The cause of focal nodular hyperplasia is not well understood. Congenital vascular malformation or vascular injury has been suggested as the underlying mechanism for hepatocellular hyperplasia.[15] It is eight times more common in females than men and most are incidentally found between the third and fifth decades. Generally, focal nodular hyperplasia presents as a solitary nodule smaller than 5 cm in diameter.[35]

FNH has a distinctive appearance on CEUS, showing an artery entering the lesion, branching, and supplying the mass centrifugally.[36] Arterial filling of FNH occurs early and rapidly, within the first 10-30 seconds of scanning, requiring a high frame rate and real-time imaging to assess the arterial filling direction.[37] At present, contrast-enhanced sonography is the only non-invasive imaging technique to show the pattern of arterial filling in these rapidly enhancing liver lesions (Figure 7).[37] A transient peripheral unenhanced zone is another finding highly suggestive of FNH. This finding may reflect the peripheral part of the lesion which does not initially enhance due to the centrifugal enhancement pattern of FNH.[37] This transient peripheral unenhanced zone is less commonly seen than centrifugal enhancement in FNH, but once seen, reliably predicts that the lesion has centrifugal filling. The identification of this zone requires enhancement of the liver surrounding the lesion in order to be perceived. Therefore, in lesions that are in a liver that enhances later than the lesion, the zone will not be appreciated.[37]

In approximately 20% of patients, a central hypoattenuating scar may be seen.[38] A central scar in FNH represents

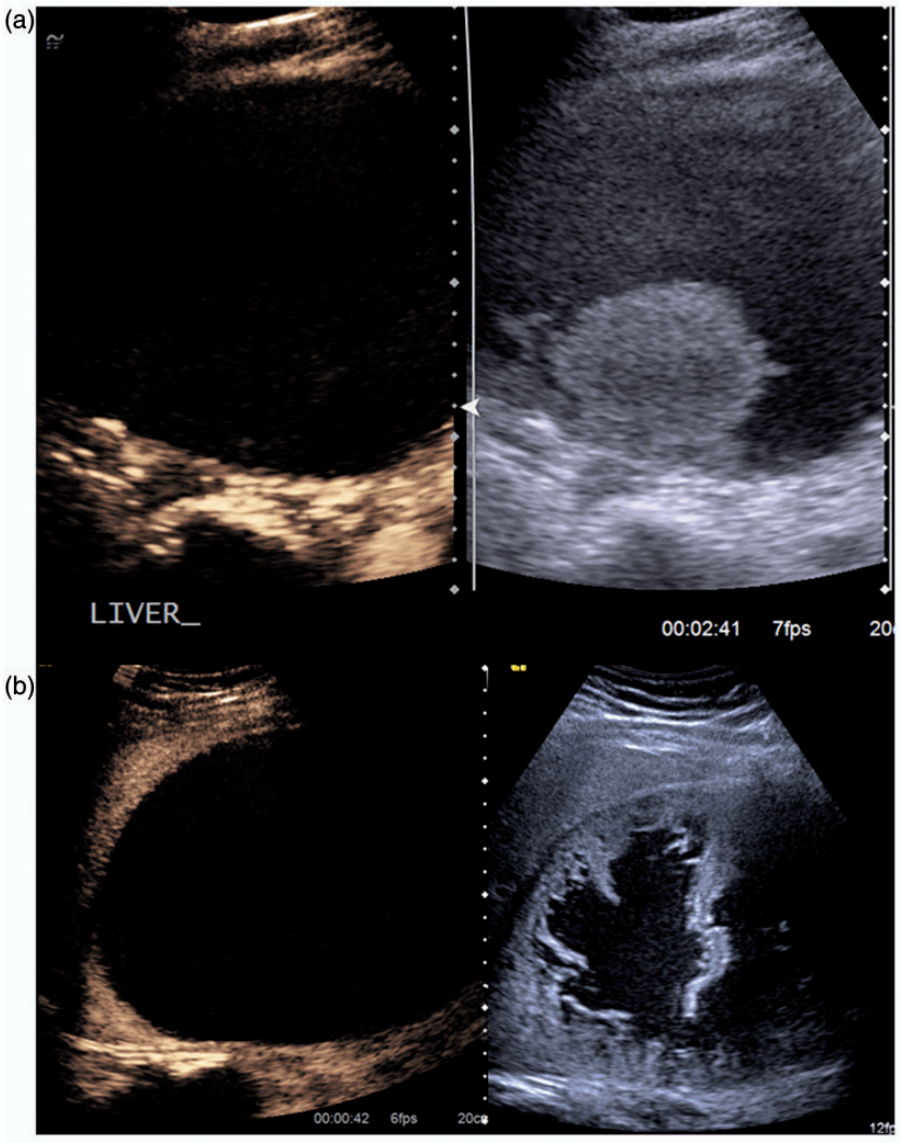

Figure 6. Hydatid cyst on: (a) grey scale and CEUS with daughter cyst and (b) peripheral septations which do not enhance post-contrast

fibrous connective tissue radiating from its centre. A central scar is seen as a stellate non-enhancing area, best visualised in the extended observation of the portal venous phase. Unlike MRI, on which a central scar shows enhancement in the delayed phase of contrast-enhanced T1-weighted imaging, no delayed enhancement is seen in the central scar on contrast-enhanced sonography. This can be explained by the strictly intravascular nature of ultrasound contrast, which is different from the MRI contrast agents that show interstitial leaks and accumulation in fibrotic tissue. Sustained enhancement of the remainder of the lesion equal to or greater than that of the normal liver during the extended observation of the portal venous phase to 5 minutes has been considered a hallmark of a benign diagnosis.[39,40]

The main differential is hepatic adenoma, and it is important to distinguish between the two, as there is a recognised increased risk of bleeding or of malignant transformation with hepatic adenoma. However, differentiation between the two can often be difficult. Unless the characteristic vascular enhancement pattern is appreciated, they both appear as hypervascular enhancing masses on cross-sectional imaging.[37] Contrast ultrasound allows both the early filling and the characteristic vascular morphology to be appreciated.

Hepatocellular adenoma

Hepatocellular adenomas are rare benign hepatic tumours that commonly occur in women who have been receiving oral contraceptives for more than 2 years.[41] They are less common than FNH and almost exclusively occur in women. They are sensitive to oestrogen and will typically grow during pregnancy. On grey scale imaging, they appear as round, iso- or hyperechoic lesions. They may be heterogeneous if they contain haemorrhage. The results of recent

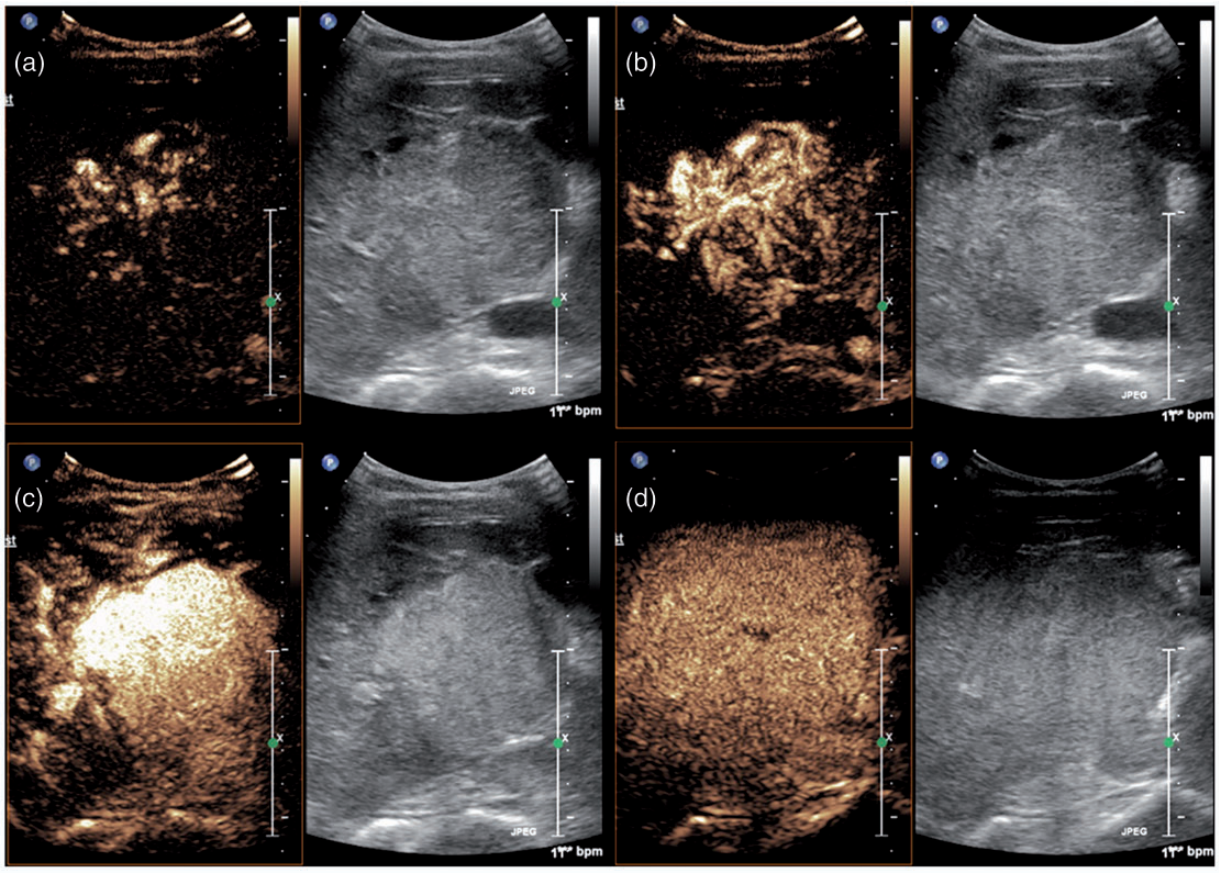

Figure 7. FNH comparative CEUS and grey-scale images showing: (a) early centrifugal filling (i.e. arterial filling away from the center of the lesion; (b) progressive, gradual filling; (c) delayed filling; (d) almost complete filling on the portovenous phase. Note the non-enhancement of the central scar

studies indicate that hepatocellular adenoma is not a single entity but a heterogeneous group of tumours characterised by specific genetic and pathologic abnormalities and tumour biology.[42] Accordingly, they display different enhancement patterns with contrast ultrasound.

The colour Doppler appearances are non-specific but large sub-capsular feeding vessels, when present, are typical. These subcapsular feeding arteries account for the centripetal blood flow of the lesion.[43] The vascularisation of an adenoma is not as fine and orderly as the pattern seen in FNH.[44] A small area of central necrosis in adenomas can be erroneously diagnosed as a central scar;[44] however, central necrosis in adenoma is irregular in shape and often has an eccentric location.

In the arterial phase there is usually complete hyperenhancement, although in some cases areas of non-enhancement may be present. Several studies have demonstrated that a number of hepatic adenomas do not enhance in the porto-venous phase, in contrast to FNH, and may show wash-out (Figure 8).[44,45]

On the basis of the genetic and pathologic features, hepatocellular adenomas are categorised into three subtypes: (a) inflammatory hepatocellular adenomas, (b) hepatocyte nuclear factor 1 α-mutated hepatocellular adenomas and (c) β-catenin-mutated hepatocellular adenomas. Different subtypes show variable clinical behaviour, imaging findings and natural history.[42]

Inflammatory hepatocellular adenoma is the most common subtype and accounts for about 40–50% of all hepatocellular adenomas. Inflammatory hepatocellular adenomas occur most frequently in young women with a history of oral contraceptive usage and in obese patients.[46] At contrast-enhanced US, inflammatory hepatocellular adenomas show arterial vascularity with centripetal filling, a peripheral rim of sustained enhancement, and central washout in the late venous phase.[47] The discrepancy between the delayed washout that is depicted on contrast-enhanced US images and is not depicted on contrast-enhanced MR images may be related to the diffusion of the gadolinium-based contrast material, but not the microbubbles, into the interstitial spaces.[47] Of all subtypes, inflammatory hepatocellular adenomas show the highest risk of bleeding, which can occur in about 30% of these tumours. About 10% of inflammatory hepatocellular adenomas show an increased risk of malignancy.[48,49]

HNF-1α-mutated hepatocellular adenomas are the second most common type of hepatocellular adenoma and constitute about 30–35% of all hepatocellular adenomas.[42] Some cases have an association with (a) maturity-onset diabetes of the young (MODY), type 3, and (b) familial

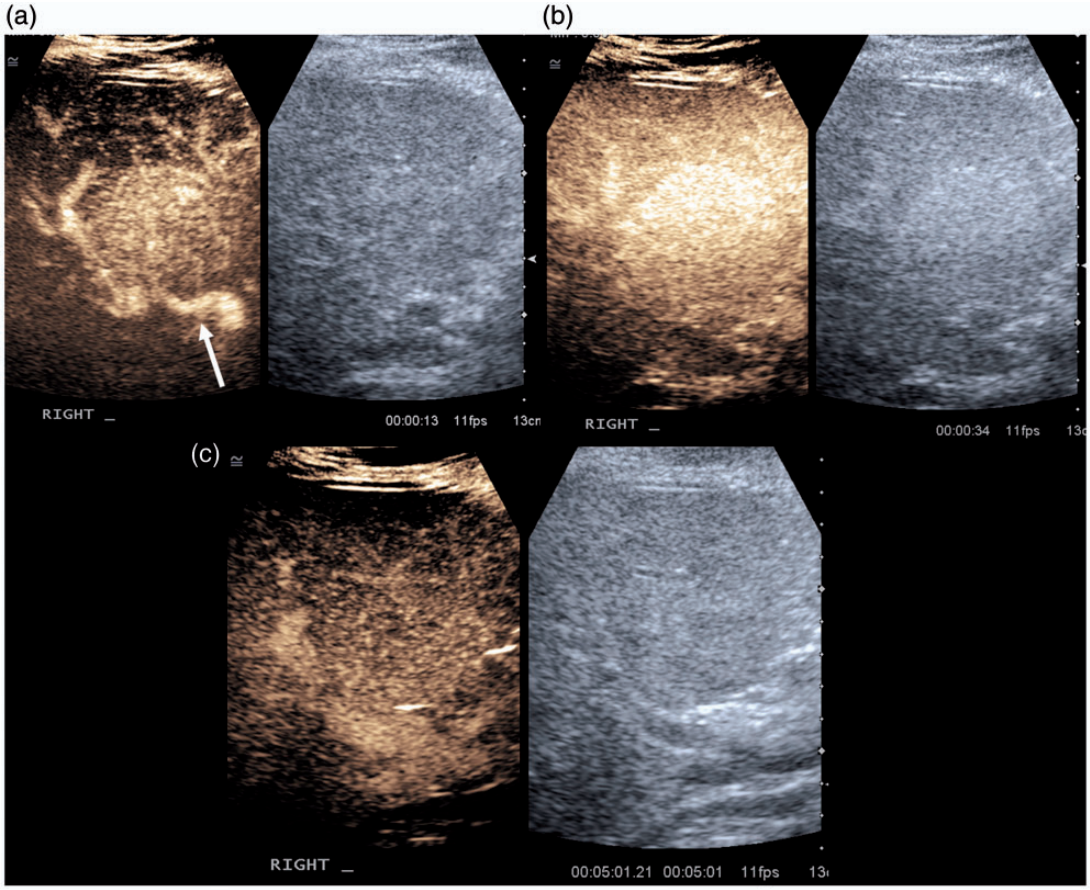

Figure 8. Hepatic adenoma. Comparative images of CEUS and grey scale (a) during the arterial phase. Note peripheral feeding vessel (white arrow) and homogenous enhancement with centripetal filling (i.e. arterial filling towards the center of the lesion). (b) Portovenous phases. Note retained contrast on the portovenous phase relative to the background liver and (c) relative wash out on the delayed image (inflammatory subtype)

hepatic adenomatosis.[48,50,51] HNF-1α-mutated hepatocellular adenomas develop exclusively in female patients, with more than 90% of patients having a history of oral contraceptive use, and the tumours are multiple in about 50% of patients. Many HNF-1α-mutated hepatocellular adenomas are asymptomatic.[42]

At contrast-enhanced US, HNF-1α-mutated hepatocellular adenomas show isovascularity to moderately increased vascularity, with mixed filling in the arterial phase after contrast material administration, and are isoechoic in the portal venous and delayed phases.[47] Among all hepatocellular adenomas, the HNF-1α-mutated hepatocellular adenomas are the least aggressive subtype: Tumours less than 5 cm in maximum dimension show minimal risk of bleeding and subsequent rupture and carry minimal or no risk for the development of malignancy.

β-Catenin-mutated hepatocellular adenomas constitute about 10–15% of all hepatocellular adenomas and are due to activating mutations of the β-catenin gene.[51] β-Catenin-mutated hepatocellular adenomas occur more frequently in men and are associated with male hormone administration, glycogen storage disease and familial adenomatosis polyposis.[46] β-Catenin-mutated hepatocellular adenomas commonly demonstrate strong arterial enhancement that may or may not persist on the portal venous and delayed phases, and these tumours may mimic hepatocellular carcinomas at imaging.[52] No specific US or multidetector CT findings for β-catenin-mutated hepatocellular adenomas have been reported in the literature.

Overall, the risk of hepatocellular carcinoma development in hepatocellular adenomas is about 5–10%.[53] The important risk factors for malignant transformation of hepatocellular adenomas are male sex, concomitant glycogen storage disease, anabolic steroid usage, the β-catenin-mutated subtype and tumours larger than 5 cm in maximum dimension.[51–53]

In certain instances, there can be overlap between the imaging characteristics of some hepatic adenomas and some small well differentiated HCCs, with both lesions demonstrating fast arterial enhancement and delayed washout. Preliminary studies suggest that whilst both lesions may be difficult to distinguish if imaging alone is used, combination with calculation of the time-intensity curve analysis maybe useful.[54]

Hepatic abscesses

Accurate diagnoses of suspected liver infections are important to determine the most effective therapy. Published reports indicate that patient mortality rates can be markedly reduced from 40% to 2% with early diagnosis and imaging-

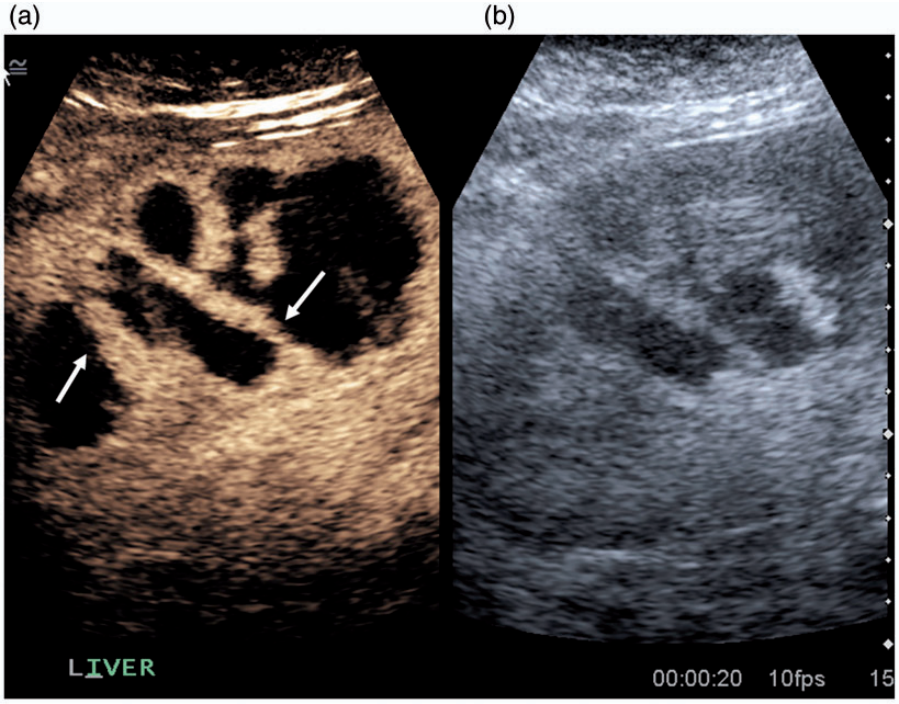

Figure 9. Hepatic abscess on: (a) CEUS and (b) grey scale demonstrating peripheral enhancement in the portovenous phase. Note the enhancing septations (arrows), which are diagnostic of abscesses. The overall size of the abscess cavity is less obvious on the grey-scale image

guided percutaneous drainage of pyogenic hepatic abscesses.[55–57]

Hepatic abscess may occur de-novo or secondary to inflammatory conditions such as appendicitis, diverticulitis or iatrogenic hepatic intervention. On B-Mode, abscesses tend to have a variable appearance depending on degree of liquefaction and loculation. They may appear inhomogeneously hypoechoic with central anechoic areas or inhomogeneously hypoechoic, but solid. They may contain gas echoes. Abscesses may be ovoid or irregular and demonstrate sharp or irregular margins. Thick irregular walls and internal echogenic debris are often seen. Colour Doppler may show peripheral flow.

On both the arterial phase and the portal-venous phase of CEUS, there is rim enhancement but no central enhancement, except for possible enhancing septa. Hyperenhancement of the adjacent liver may be identified. On the late phase, the rim tends to be hypo-enhancing and a lack of central enhancement persists (Figure 9). Lack of internal enhancement on CEUS is a characteristic enhancement pattern of pyogenic hepatic abscesses, whereas hepatic malignancies manifest as diffuse or peripheral intratumoural enhancement, with peripheral enhancement. The phenomenon of transient hyperenhanced liver parenchyma may be due to the loss of the balance between arterial and portal blood supply because of perilesional hyperemia and portal venous obstruction.[58]

Conclusion

CEUS has the ability to provide an immediate answer regarding the nature of liver lesions by determining their vascular characteristics. Contrast bubble agent is an intravascular only agent, with a high safety profile and relative low cost. Increasing awareness and education is necessary as interpretation is operator dependent. The ability to rapidly diagnose benign lesions in the ultrasound department will ensure compliance with the NICE guidelines and help to decrease patient and clinician anxiety when an incidental liver lesion has been detected.

DECLARATIONS

Competing interests: The authors have no conflicts of interest to declare.
Funding: This work received no specific grant from any funding agency in the public, commercial, or not-for-profit sectors.
Ethical approval: Not applicable.
Contributorship: SMR conceived the review and AEO and SMR researched the literature. AEO wrote the first draft and SMR wrote the final version. All authors reviewed and approved the final version of the manuscript. SMR was the project supervisor.
Acknowledgements: The authors would like to thank Professor Paul Sidhu for his advice with the manuscript and images.

REFERENCES

1. Blomley MJK, Cooke JC, Unger EC, et al. Microbubble contrast agents: a new era in ultrasound. *Brit Med J* 2001;**322**:1222–5
2. Gabata T, Matsui O, Kadoya M, et al. Aberrant gastric venous drainage in a focal spared area of segment IV in fatty liver: demonstration with color Doppler sonography. *Radiology* 1997;**203**:461–3
3. National Institute for Health and Care Excellence. *SonoVue (Sulphur Hexafluoride Microbubbles) – Contrast Agent for Contrast-enhanced Ultrasound Imaging of the Liver [DG5]*. London: National Institute for Health and Care Excellence, 2012

4. Hammer OW, Aguirre DA, Casola G, et al. Fatty Liver: imaging patterns and pitfalls. *Radiographics* 2006;**26**:1637–53
5. Glinkova V, Shevah O, Boaz M, et al. Hepatic haemangiomas: possible association with female sex hormones. *Gut* 2004;**53**:1352–5
6. Vilgrain V, Boulos L, Vullierme MP, et al. Imaging of atypical hemangiomas of the liver with pathologic correlation. *Radiographics* 2000;**20**:379–97
7. Moody AR, Wilson SR. Atypical hepatic hemangioma; a suggestive sonographic morphology. *Radiology* 1993;**188**:413–7
8. Yamashita Y, Hatanaka Y, Yamamoto H, et al. Differential diagnosis of focal liver lesions: role of spin-echo and contrast-enhanced dynamic MR imaging. *Radiology* 1994;**193**:59–65
9. Valls C, Reñe M, Gil M, et al. Giant cavernous hemangioma of the liver: atypical CT and MR findings. *Eur Radiol* 1996;**6**:448–50
10. Nelson RC, Chezmar JL. Diagnostic approach to hepatic hemangiomas. *Radiology* 1990;**176**:11–13
11. Hanafusa K, Ohashi I, Himeno Y, et al. Hepatic hemangioma: findings with two-phase CT. *Radiology* 1995;**196**:465–9
12. Jang, H-J, Kim TK, Burns, PN, Wilson SR. Enhancement patterns of hepatocellular carcinoma at contrast-enhanced ultrasound: Comparison with histologic differentiation. *Radiology* 2007;**244**:898–906
13. Matsui O, Kadoya M, Takahashi S, et al. Focal sparing of segment IV in fatty livers shown by sonography and CT: correlation with aberrant gastric venous drainage. *Am J Roentgenol* 1995;**164**:1137–40
14. Kobayashi S, Matsui O, Kadoya M, et al. CT arteriographic confirmation of focal hepatic fatty infiltration adjacent to the falciform ligament associated with drainage of inferior vein of Sappey: a case report. *Radiat Med* 2001;**19**:51–4
15. Mathieu D, Vilgrain V, Mahfouz AE, et al. Benign liver tumors. *Magn Reson Imaging Clin N Am* 1997;**5**:255–88
16. Vachha B, Sun MR, Siewert B, et al. Cystic lesions of the liver. *Am J Roentgenol* 2011;**196**:W355–66
17. vanSonnenberg E, Wroblicka JT, D'Agostino HB, et al. Symptomatic hepatic cysts: percutaneous drainage and sclerosis. *Radiology* 1994;**190**:387–92
18. Mortele KJ, Ros PR. Cystic focal liver lesions in the adult: differential CT and MR imaging features. *Radiographics* 2001;**21**:895–910
19. Powers C, Ros PR, Stoupis C, et al. Primary liver neoplasms: MR imaging with pathologic correlation. *Radiographics* 1994;**14**:459–82
20. Lev-Toaff AS, Bach AM, Wechsler RJ, et al. The radiologic and pathologic spectrum of biliary hamartomas. *Am J Roentgenol* 1995;**165**:309–13
21. Lung PF, Jaffer OS, Akbar N, et al. Appearances of von Meyenburg complex on cross-sectional imaging. *J Clin Imaging Sci* 2013;**3**:22
22. Berry JD, Boxer ME, Rashid HI, et al. Microbubble contrast-enhanced ultrasound characteristics of multiple biliary hamartomas (von Meyenberg complexes). *Ultrasound* 2004;**12**:95–7
23. Wohlgemuth WA, Bottger J, Bohndorf JB. MRI, CT, US and ERCP in the evaluation of bile duct hamartomas (von Meyenburg complex): a case report. *Eur Radiol* 1998;**8**:1623–6
24. Slone HW, Bennet WF, Bova JG.. MR findings of multiple biliary hamartomas. *Am J Roentgenol* 1993;**161**:581–3
25. Semelka RC, Hussain SM, Marcos HB, et al. Biliary hamartomas: solitary and multiple lesions shown on current MR techniques including gadolinium enhancement. *Magn Reson Imaging* 1999;**10**:196–201
26. Moguillanski SJ, Gimenez CR, Villavicencio RL. Radiología de la hidatidosis abdominal. In: Stoopen ME, Kimura K, Ros PR, eds. *Radiología e Imagen Diagnóstica y Terapeútica: Abdomen*. Vol 2. Philadelphia, PA: Lippincott Williams & Wilkins, 1999
27. Lewall DB, McCorkell SJ. Hepatic echinococcal cyst: sonographic appearance and classification. *Radiology* 1985;**155**:773–5
28. Beggs I. The radiology of hydatid disease. *Am J Roentgenol* 1985;**145**:639–48
29. von Sinner WN. New diagnostic sign in hydatid disease: radiography, ultrasound, CT and MRI correlated to pathology. *Eur J Radiol* 1990;**12**:150–9
30. Gharbi HA, Hassine W, Brauner MW, et al. Ultrasound examination of the hydatic liver. *Radiology* 2013;**139**:459–63
31. Bezzi M, Teggi A, De Rosa F, et al. Abdominal hydatid disease: US findings during medical treatment. *Radiology* 1987;**162**:91–5
32. Lewall DB. Hydatid disease: biology, pathology, imaging and classification. *Clin Radiol* 1998;**52**:863–74
33. Pedrosa I, Saíz A, Arrazola J, et al. Hydatid disease: radiologic and pathologic features and complications. *Radiographics* 2000;**20**:795–817
34. Wanless IR, Mawdsley C, Adams R. On the pathogenesis of focal nodular hyperplasia of the liver. *Hepatology* 1985;**5**:1194–200
35. Mortelé KJ, Praet M, Van Vlierberghe H, et al. CT and MR imaging findings in focal nodular hyperplasia of the liver. *Am J Roentgenol* 2000;**175**:687–92
36. Fechner RE, Roehm JO. Angiographic and pathologic correlations of hepatic focal nodular hyperplasia. *Am J Surg Pathol* 1977;**1**:217–24
37. Kim TK, Jang HY, Burns PN, et al. Focal nodular hyperplasia and hepatic adenoma: differentiation with low-mechanical-index contrast-enhanced sonography. *Am J Roentgenol* 2008;**190**:58–66
38. Shamsi K, De Schepper A, Degryse H, et al. Focal nodular hyperplasia of the liver: radiologic findings. *Abdom Imaging* 1993;**18**:2–38
39. Dietrich CF, Ignee A, Trojan J, et al. Improved characterisation of histologically proven liver tumours by contrast enhanced ultrasonography during the portal venous and specific late phase of SHU 508A. *Gut* 2004;**53**:401–5
40. Wilson SR, Burns PN. An algorithm for the diagnosis of focal liver masses using microbubble contrast-enhanced pulse-inversion sonography. *Am J Roentgenol* 2006;**186**:1401–12
41. Edmondson HA, Henderson B, Benton B. Liver-cell adenomas associated with use of oral contraceptives. *N Engl J Med* 1976;**294**:470–2
42. Katabathina VS, Menias CO, Shanbhogue AKP, et al. Genetics and imaging of hepatocellular adenomas: 2011 Update. *Radiographics* 2011;**31**:1529–43
43. Mathieu D, Bruneton JN, Drouillard J, et al. Hepatic adenomas and focal nodular hyperplasia: dynamic CT study. *Radiology* 1986;**160**:53–8
44. Ichikawa T, Federle MP, Grazioli L, et al. Hepatocellular adenoma: multiphasic CT and histopathologic findings in 25 patients. *Radiology* 2000;**214**:861–8
45. Dietrich CF, Schuessler G, Trojan J, et al. Differentiation of focal nodular hyperplasia and hepatocellular adenoma by contrast-enhanced ultrasound. *Br J Radiol* 2005;**78**:704–7
46. Bioulac-Sage P, Laumonier H, Laurent C, et al. Hepatocellular adenoma: what is new in 2008. *Hepatol Int* 2008;**2**:316–21
47. Laumonier H, Cailliez H, Balabaud C, et al. Contrast-enhanced ultrasonography to identify the two major subtypes of hepatocellular adenoma. *J Hepatol* 2010;**52**:S223
48. Bioulac-Sage P, Balabaud C, Zucman-Rossi J. Subtype classification of hepatocellular adenoma. *Dig Surg* 2010;**27**:39–45
49. Zucman-Rossi J, Jeannot E, Nhieu JT, et al. Genotype-phenotype correlation in hepatocellular adenoma: new classification and relationship with HCC. *Hepatology* 2006;**43**:515–24
50. Bioulac-Sage P, Laumonier H, Couchy G, et al. Hepatocellular adenoma management and phenotypic classification: the Bordeaux experience. *Hepatology* 2009;**50**:481–9
51. Bioulac-Sage P, Blanc JF, Rebouissou S, et al. Genotype phenotype classification of hepatocellular adenoma. *World J Gastroenterol* 2007;**13**:2649–54
52. Laumonier H, Bioulac-Sage P, Laurent C, et al. Hepatocellular adenomas: magnetic resonance imaging features as a function of molecular pathological classification. *Hepatology* 2008;**48**:808–18
53. Farges O, Dokmak S. Malignant transformation of liver adenoma: an analysis of the literature. *Dig Surg* 2010;**27**:32–8
54. Zhu XL, Chen P, Guo H, et al. Contrast-enhanced ultrasound for the diagnosis of hepatic adenoma. *J Int Med Res* 2011;**39**:920–8
55. Tazawa J, Sakai Y, Maekawa S, et al. Solitary and multiple pyogenic liver abscesses: characteristics of the patients and efficacy of percutaneous drainage. *Am J Gastroenterol* 1997;**92**:271–4
56. Giorgio A, Tarantino L, Mariniello N, et al. Pyogenic liver abscesses: 13 years of experience in percutaneous needle aspiration with US guidance. *Radiology* 1995;**195**:122–4
57. Kuligowska E, Connors SK, Shapiro JH. Liver abscess: sonography in diagnosis and treatment. *Am J Roentgenol* 2013;**138**:253–7
58. Liu GJ, Lu MD, Xie XY, et al. Real-time contrast-enhanced ultrasound imaging of infected focal liver lesions. *J Ultrasound Med* 2008;**27**:657–66